Research Article

FangMing Zhou*, DongHao Xu, MingXiao Shi, and YanHua Bi

Investigation on microstructure and its transformation mechanisms of B_2O_3-SiO_2-Al_2O_3-CaO brazing flux system

https://doi.org/10.1515/htmp-2020-0021
Received Aug 14, 2019; accepted Nov 26, 2019

Abstract: The B_2O_3-SiO_2-Al_2O_3-CaO brazing fluxes and slags were investigated by using X-ray photoelectron spectroscopy (XPS) and Fourier transform infrared spectroscopy (FTIR). The microstructure of the fluxes and slags and its transformation mechanism during the brazing process were investigated, especially the effect of ratio of $B_2O_3$to SiO_2(B_2O_3/SiO_2) on the microstructural transformation was analyzed. The results show that the structure units of the fluxes and slags are [BO_4], [BO_3], [SiO_4], [AlO_4] and [AlO_6], and the network structure is a silicon-boron network structure. The O in the slags consist of bridged oxygen, non-bridged oxygen and free oxygen. During the brazing process, part of the [BO_4] in slag combined with silica-oxygen network to form Si-O-B structure, which contribute to the network structure of slag, and another part of the [BO_4] was transformed to [BO_3]. The increase of (B_2O_3/SiO_2) contribute to the transformation of [BO_4] to [BO_3], and more B_2O_3 take part in the interface reaction with the increase of (B_2O_3/SiO_2). Therefore, the increase of (B_2O_3/SiO_2) leads to the decrease in the viscosity of the slag, which is beneficial to the spreading behavior during the brazing process.

Keywords: borosilicate; brazing flux; slag structure; FTIR; XPS

1 Introduction

In the metallurgical processes of continuous casting, steel smelting and welding, metallurgical slag plays an important role in the metallurgical reaction process [1–3]. The liquid slag can react with the molten filler metal and the chemistry of metal will be modified, and the material properties will be altered after solidification. After solidification, the slag can cover the metal surface and protect the metal from oxidation [4, 5]. The commonly used metallurgical slag system is silicate slag, such as CaO-Al_2O_3-SiO_2, TiO_2-CaO-SiO_2, MgO-CaO-SiO_2, etc. [7–9]. Slag system with B_2O_3 as main component is also often used in brazing process. In recent years, scholars have developed borosilicate slag system by adding B_2O_3 to the slag system to adjust the metallurgical properties of the slag system. Research shows that adding a certain amount of B_2O_3 in the slag system can improve the reaction kinetics conditions and regulate the reaction between slag and metal [10–13].

The microstructure of the material determines its macroscopic properties. The structure and morphology of the slag directly affect the properties of the slag and the chemical reactions of the slag with metal melts [14, 15]. Therefore, it is very important to investigate the microstructure of slag for the theoretical study of metallurgical slag system. Several research have been conducted in the study on the structure of metallurgical slag. Kim [16–18] *et al.* analyzed the effect of the composition and composition ratio of TiO_2 and SiO_2 contenting slag system on the structure by means of XPS, FTIR and Raman spectroscopy. It was concluded that the main reason for the change of the structure was the effect of the composition of the slag on the network of silicate slag and the coordination mode of complex ions. Wu [19] *et al.* studied the structure of SiO_2-Al_2O_3-Fe_2O_3 slag system. It was found that Ca^{2+} and Mg^{2+} would destroy the bridging oxygen bonds in the slag system, thus producing low melting point compounds and lowering the melting temperature of the slag system. Park [20] *et al.* studied the structure and influencing factors of CaF_2-CaO-

***Corresponding Author: FangMing Zhou:** Jiangsu Province Key Lab of Advanced Welding Technology, Jiangsu University of Science and Technology, Zhenjiang 212003, China;
Email: fangmingzhou@just.edu.cn
DongHao Xu, MingXiao Shi, YanHua Bi: Jiangsu Province Key Lab of Advanced Welding Technology, Jiangsu University of Science and Technology, Zhenjiang 212003, China

SiO_2 slag system by means of FTIR. It is considered that the structure of slag is directly related to its ability to dissolve H and O elements in weld metal.

In the study of borosilicate slag system, Wan [21] *et al.* analyzed the effect of Al_2O_3 on the structure of borosilicate by FTIR, and the change of the content of [BO_4] and [BO_3] caused by the change of the composition of molten slag. There are also scholars [22–24] studied the effect of the composition transformation of CaO-SiO_2-B_2O_3 borosilicate slag system on its structure and melting characteristics. However, there are few studies on the activity of borosilicate welding slag and the mechanism and influencing factors of the structure change. In this paper, B_2O_3-SiO_2-Al_2O_3-CaO brazing flux with different components was designed and manufactured, and the flux was used for submerged arc brazing of tin-based babbitt alloy. The microstructural characteristics of B_2O_3-SiO_2-Al_2O_3-CaO brazing flux and slag were analyzed by FTIR and XPS, and the structure transformation mechanism of the slag system was also investigated. The effect of (B_2O_3/SiO_2) on the microstructure of the slag was also explored.

2 Experimental

According to the composition of commonly used borosilicate fluxes [10–13, 21–24], the composition of brazing flux system used in the experiment is designed, and CaO and Al_2O_3 are selected as slag making agents. The main component participted in the interface reaction during brazing process of flux is B_2O_3, while CaO and Al_2O_3 do not participate in the interface reaction and have little influence on the spreading area. Therefore, flux with different (B_2O_3/SiO_2) is designed to explore its influence on the spreading area. The flux composition used in the experiment is shown in Table 1, numbered a, b, c, d. For a to d, the (B_2O_3/SiO_2) increase gradually. The raw material is weighed in proportion, grinded and mixed, dried at 200°C for 2 hours, sintered at 350°C for 2.5 hours, and finally made into flux.

The submerged arc brazing experiment was carried out with the prepared flux. The ZChSnSb11-6 tin-based babbitt with weight of 1.0g was used as brazing filler and Q235B steel plate with size of 60mm*60 mm*10 mm was used as base metal in the experiment. The parameters of submerged arc brazing are shown in Table 2. Slag is collected after brazing and the chemical composition of slag was determined by X Ray Fluorescence (XRF, EDX-7000), and the result is shown in Table 3. These values are the average of at least three measurements and the standard deviation is also provided within the table.

Table 1: Chemical constitution of slag system(wt.%)

Samples	B_2O_3	SiO_2	Al_2O_3	CaO
a	30	32.5	22.5	15
b	30	30	23.5	16.5
c	30	27.5	25	17.5
d	30	25	26	19

Table 2: Parameters of submerged arc brazing

Flux thickness	current	Arc length	Brazing time
30mm	180A	6mm	2s

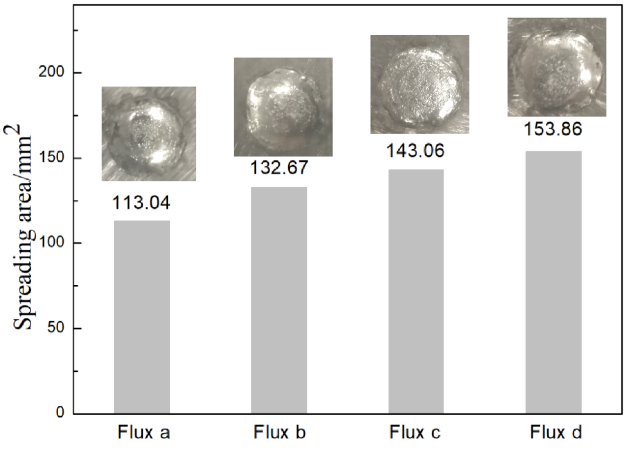

Figure 1: Spreading area of submerged arc brazing tin-based babbitt

Temperature distributions in the brazing area were measured with thermocouples. The results show that under the experiment parameters, the maximum temperature in the medal of the brazing area is about 1500 K and the maximum temperature in the edge of the brazing area is about 600 K. The spreading area for different fluxes was measured, with the results shown in Figure 1. It can be seen from the figure that the spreading area increases with the increase of the ratio of (B_2O_3/SiO_2). Fourier transform infrared spectroscopy (FTIR, Cary670) was used to detect the vibration of each structural groups in flux and slag. X-ray photoelectron spectroscopy (XPS, Escalab 250Xi) was used to analyze the Si, B and O elements in flux and slag.

Table 3: XRF result of slag (wt.%)

Slag	B_2O_3	SiO_2	Al_2O_3	CaO	SnO_2	Fe_2O_3	Sb_2O_3	CuO
a	28.37 (±0.181)	33.46 (±0.1751)	21.57 (±0.284)	13.62 (±0.181)	2.41 (±0.181)	0.22 (±0.042)	0.24 (±0.017)	0.11 (±0.031)
b	30.42 (±0.367)	30.75 (±0.161)	21.07 (±0.121)	14.12 (±0.154)	2.75 (±0.197)	0.49 (±0.048)	0.38 (±0.036)	0.09 (±0.012)
c	31.95 (±0.215)	25.75 (±0.138)	22.73 (±0.292)	15.34 (±0.039)	3.29 (±0.214)	0.47 (±0.035)	0.34 (±0.019)	0.13 (±0.015)
d	31.82 (±0.284)	23.31 (±0.154)	23.76 (±0.341)	17.06 (±0.124)	3.15 (±0.212)	0.51 (±0.027)	0.27 (±0.064)	0.12 (±0.017)

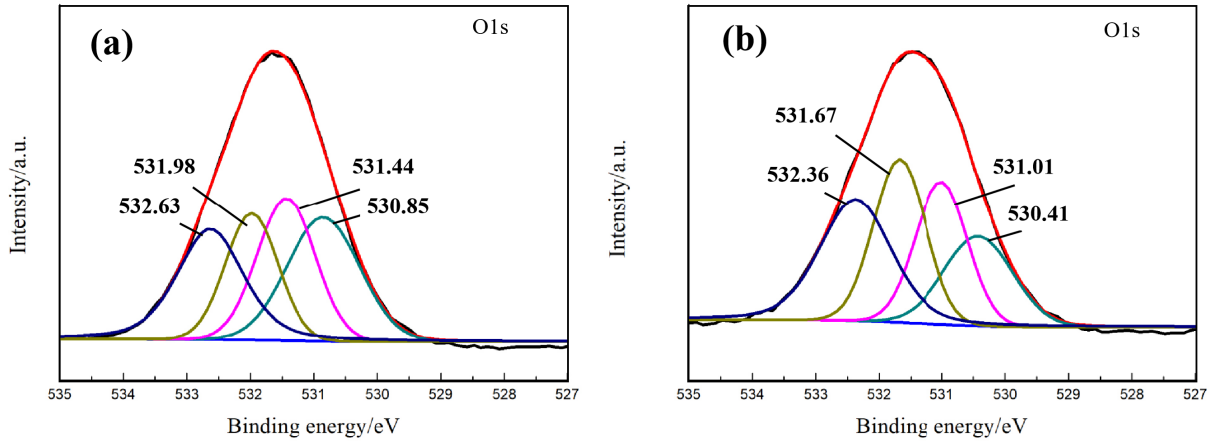

Figure 2: XPS peak differentation imitating analysis of O(1s): a) flux, b) slag

3 Results and discussion

3.1 Investigation on microstructure of flux and slag using XPS

To analyze the structure of the B_2O_3-SiO_2-Al_2O_3-CaO slag system and its transformation mechanism during brazing process, the brazing flux and slag was analyzed using XPS and the peak fitting of O, B and Si was carried out. According to the existing research results [16–18], the change of components proportion of a certain flux system has little effect on its structure transformation mechanism from flux to slag, but only on the content of structural group. Therefore, the XPS results of flux a in Table 1 was selected for specific analysis and discussion about the transformation mechanism from flux to slag during brazing process. The results were shown in Figure 2, 3 and 4 and Table 4 and 5.

The analysis results of the peaks of O(1s) are shown in Figure 2. It can be seen from the figure that there are four forms of O in both flux and slag. The main forms of O are bridged oxygen, non-bridged oxygen and free oxygen. The corresponding binding energies are non-bridged oxygen (530 ± 0.5 eV), bridged oxygen (531.8 ± 0.3 eV), oxygen in alumina (531.1 ± 0.3 eV) and Oxygen in silica (532.65 ± 0.3 eV). It is found that the main change in the form of O element during the transformation from flux to slag is the change between non-bridged oxygen and bridged oxygen. In the slag, the bridged oxygen increases significantly, while the non-bridged oxygen decreases significantly.

The analysis results of B(1s) are shown in Figure 3. It can be seen from the figure that there are two main forms of B, which belong to two different coordination modes of B element, corresponding to four coordination [BO_4] (192.5 eV ± 0.5 eV) and three coordination [BO_3] (191.8 ± 0.4 eV). According to the analysis results, it can be seen that, compared with flux, [BO_3] in slag increases significantly while [BO_4] in slag decreases accordingly, which indicates that the coordination form of B element has changed partly in the transformation process of flux to slag.

The analysis results of Si(2p) are shown in Figure 4. It can be seen from the figure that the Si elements exist mainly in two forms in flux and slag. That are bridged oxygen silicon, corresponding binding energy (103 ± 0.4 eV) and non-bridged oxygen silicon, corresponding binding energy (102.4 ± 0.4 eV). It can be found that the con-

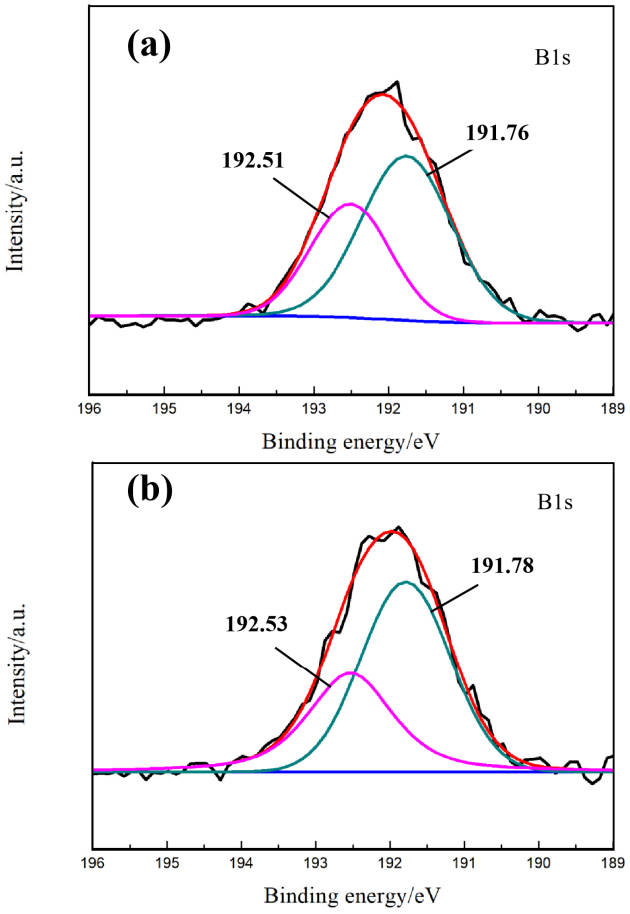

Figure 3: XPS peak differentation imitating analysis of B(1s): a) flux, b) slag

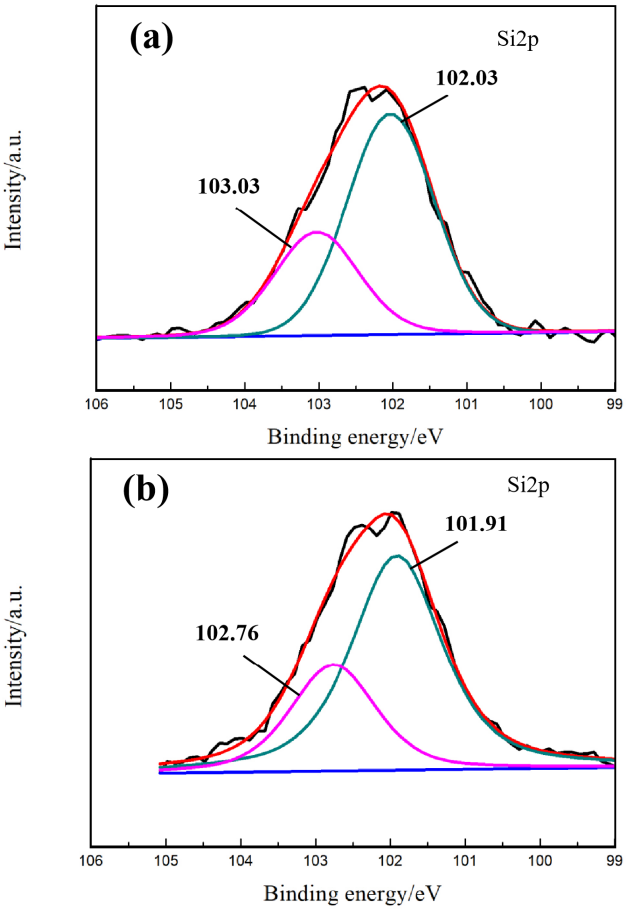

Figure 4: XPS peak differentation imitating analysis of Si(2p): a) flux, b) slag

Table 4: XPS analysis of flux

Elements	Peak	Position	FWHM	Area
O(1s)	1	530.85	1.35	28424.52
	2	531.44	1.08	26132.4
	3	531.98	0.97	20928.68
	4	532.63	1.21	27183.26
B(1s)	1	191.76	1.41	3889.933
	2	192.51	1.25	2341.192
Si(2p)	1	102.03	1.39	4287.845
	2	103.03	1.35	2064.132

Table 5: XPS analysis of slag

Elements	Peak	Position	FWHM	Area
O(1s)	1	530.41	1.28	12955.46
	2	531.01	0.98	15879.08
	3	531.67	0.97	17974.4
	4	532.36	1.31	20445.99
B(1s)	1	191.78	1.41	2218.579
	2	192.53	1.33	1376.172
Si(2p)	1	101.91	1.43	3736.931
	2	102.76	1.34	1629.661

tent of non-bridged oxygen silicon is higher than that of bridged oxygen silicon in both flux and slag, while the content of bridged oxygen silicon and non-bridged oxygen silicon show no obvious change between slag and flux.

3.2 Investigation on microstructure of flux and slag using FTIR

FTIR was used to investigate the structure of B_2O_3-SiO_2-Al_2O_3-CaO brazing flux and slag with different ratio of (B_2O_3/SiO_2) in composition. Table 6 lists the absorption zones of the main groups in the slag system according to the relevant literature [16–18, 20, 25, 26]. Figure 5 is a com-

Table 6: Main Vibration Types and Their Absorption Bands

Wavenumbers / cm^{-1}	Assignment
460	Bending vibration of Si—O—Si
500-600	asymmetric stretching vibration of $[AlO_6]$-octahedron
700	Bending vibration of $[BO_3]$
778-798	asymmetric Stretching vibration of $[AlO_4]$
820	symmetric stretching vibration of Si—O—Si
~900	B-O bond in $[BO_4]$ units from diborate groups
1020-1060	asymmetric stretching vibration of Si—O—Si
1200-800	Stretching vibration of $[BO_4]$
950-1080	asymmetric stretching vibration of Si—O—B
1400	Stretching vibration of $[BO_3]$

parison of FTIR spectra between flux and slag. It can be seen from the spectra that the structure of the slag is approximately the same as that of flux. The main structure units of the slag system include $[SiO_4]$, $[BO_4]$ and $[BO_3]$. The $[BO_3]$ bending vibration in slag, which is observed in the wavenumber of 700 cm^{-1}, becomes more pronounced compared with flux. And the $[BO_3]$ stretching vibration in slag, which is observed in the wavenumber of 1400 cm^{-1}, becomes more pronounced compared with flux too. This suggests that the content of $[BO_3]$ in the slag system increased significantly during the brazing process.

By analyzing the spectrum in the range of 800-1200 cm^{-1}, it can be found that there are obvious absorption peaks in the spectrum of flux and at the same time, there are obvious small absorption peaks near 820 cm^{-1} and 900 cm^{-1}. While in the spectrum, there is a strong absorption peak in the range of 800-1200 cm^{-1}. According to the relevant data, it can be inferred that the absorption peak near 820 cm^{-1} belongs to the stretching vibration peak of Si-O-Si bridging oxygen structure, while the absorption peak near 900 cm^{-1} belongs to the absorption peak of B-O structure in borate group, which mainly comes from the borax in flux. However, in the range of 800-1200 cm^{-1}, there are also the stretching vibration peaks of $[BO_4]$ structure, the asymmetric stretching vibration peaks of Si-O-Si structure and Si-O-B structure. Therefore, the absorption peaks in the range of 800-1200 cm^{-1} belong to the superposition peaks of $[BO_4]$ structure and bridging oxygen structure. Compared with the spectrum of flux, the absorption peaks

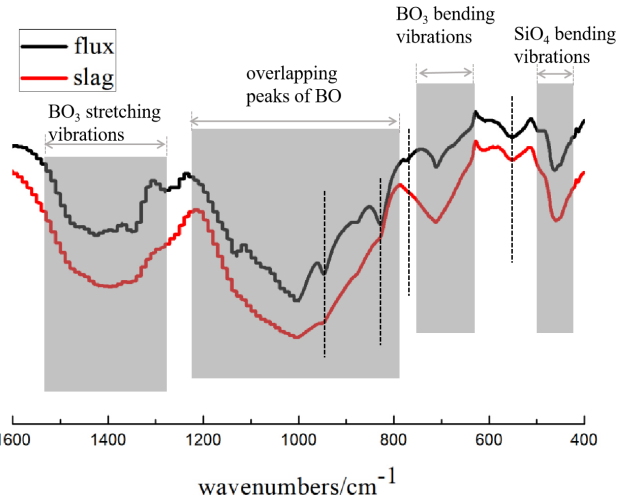

Figure 5: FTIR spectra of flux and slag

in the range of 800-1200 cm^{-1} are enhanced, while the absorption peaks near 820 cm^{-1} and 900 cm^{-1} are no longer obvious. It can be inferred that the increase of absorption peak in the range of 800-1200 cm^{-1} in slag is caused by the significant increase of Si-O-B structure, while the B-O structure of $[BO_4]$ in borate group decreases and the Si-O-Si structure decreases. This indicates that the coordination modes of B in boric acid has changed during melting, and the structure of Si-O network has also changed. The results also suggest that the coordination modes of some B has changed during brazing process, which appears as $[BO_4]$ structure transformed to $[BO_3]$ structure. At the same time, $[BO_4]$ structure enters into the Si-O network structure, forming a large number of Si-O-B bridging oxygen structure and constituting the main structure of slag.

For slag systems with different (B_2O_3/SiO_2) ratios, the FTIR spectra of slag are shown in Figure 6. By analyzing the spectra, it can be found that the absorption peaks of a, b, c and d are basically the same in position and shape. It shows that the change of the ratio of (B_2O_3/SiO_2) in slag system has no effect of generating new structure units as well as resulting in the loss of the structure units. But due to obvious change of strength of the spectrum, the (B_2O_3/SiO_2) ratio has changed the structure formation of the slag, which is reflected in the content of different structure units in the slag system.

Comparing the spectra of slag system with different (B_2O_3/SiO_2), and combining with the data in Table 2, it can be seen that with the increase of (B_2O_3/SiO_2) the absorption peaks at 1400 cm^{-1} and 700 cm^{-1} show a significant enhancement trend, and the higher the (B_2O_3/SiO_2), the more obvious the increase trend. This indicates that the increase of (B_2O_3/SiO_2) will lead to a significant in-

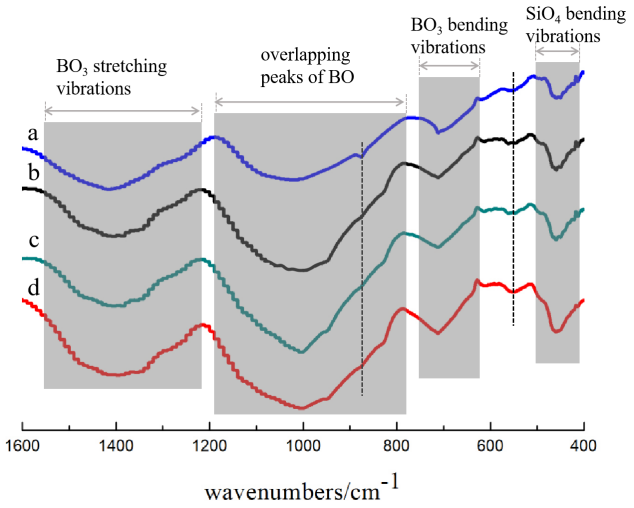

Figure 6: FTIR spectra of slag with different (B_2O_3/SiO_2)

crease in the content of [BO_3] structure in the slag. In addition, the absorption peaks in the range of 800-1200 cm^{-1} also show an increasing trend with the increase of the ratio of (B_2O_3/SiO_2), which indicates that the increase of (B_2O_3/SiO_2) will promote the formation of Si-O-B.

At the same time, by comparing the absorption peaks in the range of 500-600 cm^{-1}, it can be found that the absorption peaks gradually increase with the increase of (B_2O_3/SiO_2). According to the data in Table 2, the absorption peaks are the asymmetric stretching vibration of [AlO_6]-octahedron. The structure of Al_2O_3 in slag mainly includes [AlO_4] and [AlO_6]. The results show that [AlO_6] structure will increase with the increase of (B_2O_3/SiO_2).

3.3 Structure transformation mechanism of B_2O_3-SiO_2-Al_2O_3-CaO slag system

During the brazing process, brazing flux melts under the high temperature created by the arc and then covering the molten tin-based babbitt. B_2O_3 in flux will react with the oxides on the surface of the base metal and tin-based babbitt, which is mainly consist of oxides of Fe and Sn. After the arc is extinguished, the slag solidifies to form a slag shell and covers the brazing tin-based babbitt. The specific reactions are as follows:

$$FeO + B_2O_3 \longrightarrow Fe(BO_2) \quad (1)$$

$$2Fe_2O_3 + 3B_2O_3 \longrightarrow 2Fe_2O_3 \cdot 3B_2O_3 \quad (2)$$

$$SnO_2 + 2B_2O_3 \longrightarrow Sn(BO_2)_4 \quad (3)$$

$$CaO + B_2O_3 \longrightarrow Ca(BO_2)_2 \quad (4)$$

The oxide-film on the base metal and filler metal will hinder the spreading process. Under the effect of brazing flux, the oxides will be removed by the reaction between B_2O_3 and oxides and the reaction products dissolved in slag, as a result, the spreading of tin-based babbitt will be benefited.

Under the effect of reaction (1) – (4), the content of free oxygen [O] in the slag increases. The free oxygen [O] will interact with the original bridging oxygen structure in the slag and destroy the original Si-O and B-O bridging oxygen structure. At the same time, because B_2O_3 transferred into borate after participating in the reaction, the dispersed [BO_4] and [BO_3] increase.

According to the analysis of the first two sections, the transformation of B-containing structure which is mainly reflected in the transition from [BO_4] structure to [BO_3] structure, and the process is shown in Figure 7. In molten slag, due to the action of high temperature and existence of Ca^{2+}, a B-O bond will break in [BO_4], thus losing an [O] and became a [BO_3] structure.

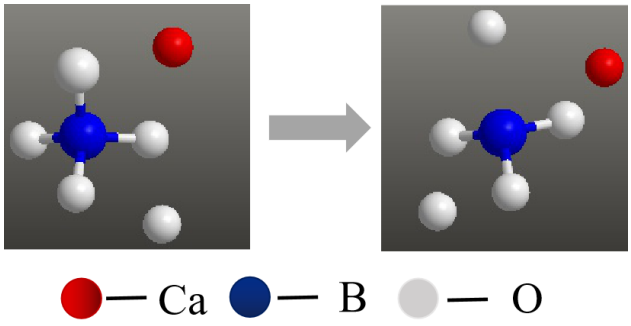

Figure 7: Diagram of transition process from [BO_4] to [BO_3]

In addition, the increase of bridging oxygen structure is mainly due to the combination of [BO_4] structure and silicon oxygen network structure to form Si-O-B structure, the process is shown in Figure 8. With the increase of (B2O3 / SiO2), the content of free [BO_4] gradually increased, so the Si-O-B structure constructed increased gradually.

The increase of bridging oxygen structure will promote the integrity of slag structure. On the one hand, the polymerization degree of slag decreases. For metallurgical slag, it can fully cover the molten metal and protect the molten metal. On the other hand, it can enhance the bonding degree of slag, and it is benefit to reduce the sticky slag on the metal surface. With the increase of (B_2O_3/SiO_2), the bonding between silica-oxygen network structure and [BO_4] is saturated gradually, and the free [BO_4] which does not bond with silica-oxygen network structure is increasing

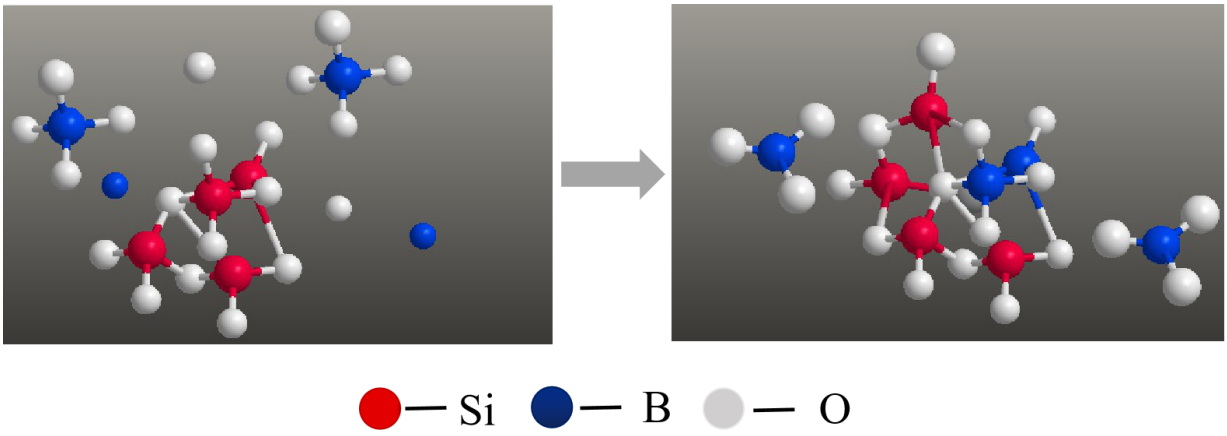

Figure 8: Process diagram of [BO_4] combined with silicon-oxygen network structure

gradually. Therefore, more B_2O_3 will participate in the interface reaction, which will lead to the enhancement of the removal effect of flux on the oxide film on the surface of base metal and filler. The hindrance to the wetting and spreading of tin-based babbitt on the base metal decreased, and the spreading area increased as a result.

With the increase of (B_2O_3/SiO_2) there are more [BO_4] which will transformed to [BO_3], and as a result the [BO_3] structure in slag increases gradually. [BO_3] is a triangular plane structure, compared with the [BO_4] with cubic tetrahedral structure, [BO_3] structure is more fluid and the increase of [BO_3] will decrease the viscosity of the slag. Because of the decrease of slag viscosity, the fluidity of the slag on the surface of base metal increased and it will also be beneficial to the spreading of tin-based babbitt covered by slag on the surface of base metal.

4 Conclusion

1. This paper investigate the microstructure of B_2O_3-SiO_2-Al_2O_3-CaO brazing flux system, and analyzed the structure transformation mechanism of the slag system from flux to slag. The main forms of O are bridged oxygen, non-bridged oxygen and free oxygen, the main forms of B are two different coordination modes which are [BO_4] and [BO_3], and the forms of Si are bridged oxygen silicon and non-bridged oxygen silicon. Compared with the structure of flux, bridged oxygen increased significantly and the proportion of structure [BO_3] increased in slag. During the brazing process, part of [BO_4] in slag combined with silica-oxygen network to form Si-O-B structure, and another part was transformed to [BO_3].
2. According to the results of submerged arc brazing experiments, the spreading area increase with the increase of (B_2O_3/SiO_2) in brazing flux system. With the increase of (B_2O_3/SiO_2), the free [BO_4] which does not bond with silica-oxygen network structure is increasing gradually. Therefore, more B_2O_3 will be involved in the interface reaction, and the effect of flux on the removal of oxide film on the surface of base metal and filler will be enhanced, which will lead to the decrease of the hindrance to the wetting and spreading of tin-based babbitt on the surface of base metal and the increase of spreading area. With the increase of (B_2O_3/SiO_2), there are more [BO_4] which will transformed to [BO_3], and as a result the [BO_3] structure in slag increases gradually. As a result, the viscosity of the slag decreased, which will be beneficial to the spreading of the tin-based babbitt covered by the slag on the surface of the base metal.

Funding: The project was supported by the Science Research Project of Jiangsu Province, China (No.15KJA460006).

References

[1] Hooli, P. Mould Flux Film between Mould and Steel Shell - Effect on Heat Flux and Defect Formation. *Steel Research International,* Vol. 74, No. 8, 2003, pp. 480–484.

[2] Fu, X., G. Wen, Q. Liu, P. Tang, J. Li, and W. Li. Development and evaluation of CaO–SiO_2 based mould fluxes for casting high aluminum trip steel. *Steel Research International,* Vol. 86, No. 2, 2015, pp. 110–120.

[3] Takeuchi, E., and J. K. Brimacombe. Effect of oscillation-mark formation on the surface quality of continuously cast steel slabs.

Metallurgical and Materials Transactions. B, Process Metallurgy and Materials Processing Science, Vol. 16, No. 3, 1985, pp. 605–625.

[4] Kanjilal, P., T. K. Pal, and S. K. Majumdar. Combined effect of flux and welding parameters on chemical composition and mechanical properties of submerged arc weld metal. *Journal of Materials Processing Technology*, Vol. 171, No. 2, 2006, pp. 223–231.

[5] Matsushita, M., and S. Liu. Hydrogen control in steel weld metal by means of fluoride additions in welding flux. *Welding Journal*, Vol. 79, No. 10, 2000, pp. 295S–303S.

[6] Gangqiang F, Jie D, Xuewei L, Effect of basicity on the crystallization behavior of TiO_2-CaO-SiO_2 ternary system slag. Cryst Eng. Comm., http://pubs.rsc.org/en/content/articlepdf/2018/ce/c8ce01078a

[7] Fan, G., J. Dang, X. Lv, M. Hu. Effect of basicity on the crystallization behavior of TiO_2-CaO-SiO_2 ternary system slag. *CrystEngComm*, Vol. 20, No. 36, 2018, pp. 5422–5431.

[8] Ren, Y., L. Zhang, Y. Zhang. Modeling reoxidation behavior of Al-Ti-containing steels by CaO-Al_2O_3-MgO-SiO_2 slag. *Journal of Iron and Steel Research International*, Vol. 25, No. 2, 2018, pp. 146–156.

[9] Kansal, I., D. U. Tulyaganov, M. J. Pascual, L. Gremillard, A. Malchere, and J. M. F. Ferreira. Sintering behaviour of diopside ($CaO{\cdot}MgO{\cdot}2SiO_2$)–fluorapatite ($9CaO{\cdot}3P_2O_5{\cdot}CaF_2$) bioactive glass. *Journal of Non-Crystalline Solids*, Vol. 380, 2013, pp. 17–24.

[10] Yu, X., Q. Shi, R. Zhai, Z. Zhu, L. Chen and Q. Luan. Influence of B_2O_3 on Melting Characteristics of CaO-Al_2O_3-SiO_2-MgO-CaF_2 Pentary Slag Series. *Special Steel*, Vol. 27, No. 4, 2006, pp. 5–7.

[11] Hamano T, Tsukihashi F. The Effect of B_2O_3 on Dephosphorization of Molten Steel by FeOx-CaO-MgOsatd.-SiO_2 Slags at 1873K. *ISIJ International*, Vol. 45, No. 2, 2005, pp. 159–165.

[12] Raiber, D. I. K., D. I. J. Hantusch, P. Hammerschmid, and D. Janke. Development of a new ceramic inclusion separator for steel melts. *Steel*

[13] Cai, Z., B. Song, L. Li, Z. Liu, and X. Cui. Effects of B_2O_3 on Viscosity, Structure, and Crystallization of Mold Fluxes for Casting Rare Earth Alloyed Steels. *Metals*, Vol. 8, No. 10, 2018, pp. 737–748.

[14] Natalie, C. A., D. L. Olson, and M. Blander. Physical and Chemical Behavior of Welding Fluxes. *Annual Review of Materials Research*, Vol. 16, No. 1, 1986, pp. 389–413.

[15] Kanjilal, P., T. K. Pal, and S. K. Majumdar. Combined effect of flux and welding parameters on chemical composition and mechanical properties of submerged arc weld metal. *Journal of Materials Processing Technology*, Vol. 171, No. 2, 2006, pp. 223–231.

[16] Kim, J. B., J. K. Choi, I. W. Han, and I. Sohn. High-temperature wettability and structure of the TiO_2–MnO–SiO_2–Al_2O_3 welding flux system. *Journal of Non-Crystalline Solids*, Vol. 432, 2016, pp. 218–226.

[17] Kim, J. B., and I. Sohn. Influence of TiO_2/SiO_2 and MnO on the viscosity and structure in the TiO_2–MnO–SiO_2 welding flux system. *Journal of Non-Crystalline Solids*, Vol. 379, 2013, pp. 235–243.

[18] Kim, J. B., and I. Sohn. Effect of SiO_2/Al_2O_3 and TiO_2/SiO_2 Ratios on the Viscosity and Structure of the TiO_2–MnO–SiO_2–Al_2O_3 Welding Flux System. *ISIJ International*, Vol. 54, No. 9, 2014, pp. 2050–2058.

[19] Wu, C. L., B. B. Wang, R. Tao, L. W. Fang, and H. X. Li. Study of Mineral Structure Transformation of Coal Ash with High Ash Melting Temperature by XPS. *Guangpuxue Yu Guangpu Fenxi*, Vol. 38, No. 7, 2018, pp. 2296–2301.

[20] Park, J. Y., W. S. Chang, and I. Sohn. Effect of MnO to hydrogen dissolution in CaF_2–CaO–SiO_2 based welding type fluxes. *Science and Technology of Welding and Joining*, Vol. 17, No. 2, 2012, pp. 134–140.

[21] Wan, J. P., J. S. Cheng, P. Lu. Effect of Al_2O_3 on the thermal expansion and phase separation of borosilicate glass. *Journal of the Chinese Ceramic Society,* Vol. 36, No. 4, 2008, pp. 544–547+551.

[22] Zhang, T. W., H. M. Wang, G. R. Li, X. Y. Zhang. Effect of B_2O_3 substituted for CaF_2 as fluxing agent on melting temperature of converter slag. *Advanced Materials Research*, Vol. 538-541, 2012, pp. 2203–2206.

[23] Wang, H. M., G. R. Li, X. Zhu, Y. T. Zhao. Research on Activities of CaO-SiO_2-B_2O_3 (Al_2O_3, Fe_2O_3) Slag System. *Applied Mechanics and Materials*, Vol. 217-219, 2012, pp. 492–495.

[24] Yang, L. L., H. M. Wang, X. Zhu, G. R. Li. Research on the Melting Temperature of CaO-SiO_2-B_2O_3 Ternary Slag Systems. *Key Engineering Materials*, Vol. 575-576, 2013, pp. 370–373.

[25] Gu, S., Z. Wang, S. Jiang, and H. Lin. Influences of Fe_2O_3 on the structure and properties of Bi_2O_3–B_2O_3–SiO_2 low-melting glasses. *Ceramics International*, Vol. 40, No. 5, 2014, pp. 7643–7645.

[26] Sun, Y., J. Liao, K. Zheng, X. Wang, and Z. Zhang. Effect of B_2O_3 on the Structure and Viscous Behavior of Ti-Bearing Blast Furnace Slags. *JOM*, Vol. 66, No. 10, 2014, pp. 2168–2175.